Characterizing the consistency of motion of spermatozoa through nanoscale motion tracing

Sunil Bhatt, Ph.D.,[a] Ankit Butola, Ph.D.,[b] Sebastian Acuña, Ph.D.,[b] Daniel Henry Hansen, M.Sc.,[b] Jean-Claude Tinguely, Ph.D.,[b] Mona Nystad, Ph.D.,[c,d] Dalip Singh Mehta, Ph.D.,[a] and Krishna Agarwal, Ph.D.[b]

[a] Bio-photonics and Green-photonics Laboratory, Department of Physics, Indian Institute of Technology Delhi, Hauz-Khas, New Delhi, India; [b] Department of Physics and Technology, UiT The Arctic University of Norway, Tromsø, Norway; [c] Department of Clinical Medicine, Women's Health and Perinatology Research Group, UiT The Arctic University of Norway, Tromsø, Norway; and [d] Department of Obstetrics and Gynecology, University Hospital of North Norway, Tromsø, Norway

Objective: To demonstrate nanoscale motion tracing of spermatozoa and present analysis of the motion traces to characterize the consistency of motion of spermatozoa as a complement to progressive motility analysis.
Design: Anonymized sperm samples were videographed under a quantitative phase microscope, followed by generating and analyzing superresolution motion traces of individual spermatozoa.
Setting: Not applicable.
Patient(s): Centrifuged human sperm samples.
Intervention(s): Not applicable.
Main Outcome Measure(s): Precision of motion trace of individual sperms, presence of a helical pattern in the motion trace, mean and standard deviations of helical periods and radii of sperm motion traces, speed of progression.
Result(s): Spatially sensitive quantitative phase imaging with a superresolution computational technique MUltiple SIgnal Classification ALgorithm allowed achieving motion precision of 340 nm using $\times 10$, 0.25 numerical aperture lens whereas the diffraction-limited resolution at this setting was 1,320 nm. The motion traces thus derived facilitated new kinematic features of sperm, namely the statistics of helix period and radii per sperm.

Through the analysis, 47 sperms with a speed >25 μm/s were randomly selected from the same healthy donor semen sample, it is seen that the kinematic features did not correlate with the speed of the sperms. In addition, it is noted that spermatozoa may experience changes in the periodicity and radius of the helical path over time. Further, some very fast sperms (e.g., >70 μm/s) may demonstrate irregular motion and need further investigation.

Presented computational analysis can be used directly for sperm samples from both fertility patients with normal and abnormal sperm cell conditions.

We note that MUltiple SIgnal Classification ALgorithm is an image analysis technique that may vaguely fall under the machine learning category, but the conventional metrics for reporting found in Enhancing the QUAlity and Transparency Of health Research network do not apply. Alternative suitable metrics are reported, and bias is avoided through random selection of regions for analysis. Detailed methods are included for reproducibility.
Conclusion(s): Kinematic features derived from nanoscale motion traces of spermatozoa contain information complementary to the speed of the sperms, allowing further distinction among the progressively motile sperms. Some highly progressive spermatozoa may have irregular motion patterns, and whether irregularity of motion indicates poor quality regarding artificial insemination needs further investigation. The presented technique can be generalized for sperm analysis for a variety of fertility conditions. (F S Sci® 2024;5: 215–24. ©2024 by American Society for Reproductive Medicine.)
Key Words: Assisted reproduction, sperm cells, computer-assisted sperm analysis, beyond progressive motility, sperm selection

Received February 20, 2024; revised June 23, 2024; accepted July 3, 2024.
S.B. and A.B. should be considered similar in author order.
Supported by the H2020-funded European Research Council Starting Grant project 3D-nanoMorph (ID: 804233) and Horizon Europe-funded European Research Council Proof of Concept project Spermotile (ID: 101123485), both at UiT The Arctic University of Norway, Tromsø, Norway.
S.B.'s mobility was partially supported by the Research Council of Norway's project ID: 309802 at UiT The Arctic University of Norway, Tromsø, Norway.
Data availability: The data generated in this research letter will not be made publicly available. However, interested users can contact the authors to discuss data sharing, usage, and reporting.
Correspondence: Krishna Agarwal, Ph.D., Department of Physics and Technology, UiT The Arctic University of Norway, #03.28, Teknologibygget, Klokkargårdsbakken 35, 9019 Tromsø, Norway (E-mail: krishna.agarwal@uit.no).

F S Sci® Vol. 5, No. 3, August 2024 2666-335X

https://doi.org/10.1016/j.xfss.2024.07.002

Assisted reproduction technologies (ARTs) have imparted freedom, choice, and opportunity to human beings in terms of reproduction. Assisted reproduction technologies for fertilization i.e., forming an embryo from a female's egg and a male's sperm fall into three solutions – intrauterine insemination (1), in vitro fertilization (IVF) (2), and intracytoplasmic sperm injection (ICSI) (3). Interestingly, intrauterine insemination, IVF, and ICSI have one common step – filtration of male's semen sample to improve its quality. In the past, several studies have been published revealing the dynamics and morphological information about sperm cells to better understand the cell-to-cell, cell-to-surface interactions, accessing the effect of real environment (4, 5). In these studies, in vivo environment is modeled in vitro by confinement using a solid flat surface. In addition, a variety of techniques have been developed to aid sperm selection (6–8), but optical microscopy-based techniques such as computer-aided semen analysis (CASA) are being increasingly preferred for ICSI. Conventional bright field and phase contrast microscopy are the core microscopy techniques used for CASA (9, 10). These techniques offer contrast because of the local refractive index variation of the sample. However, intensity maps generated from these methods are qualitative and diffraction-limited. In other words, these techniques are unable to extract nanoscale intracellular morphology which limits the detailed analysis of motility of the sperm cells. On the other hand, subdiffraction motion analysis has the potential to offer a completely different dimension to analyze the motility at the nanoscale, which may help in deriving the best quality of sperm samples for ART.

Quantitative phase imaging (QPI) is increasingly being used for sperm analysis as a high contrast label-free morphological imaging (11, 12) and identifying healthy cells from unhealthy ones (13, 14). On the other hand, Agarwal and Macháň (15) developed a superresolution technique, namely MUltiple SIgnal Classification ALgorithm (MUSICAL) (16, 17), that can trace the motion of fluorescently labeled point-like such as vesicles (18, 19). MUltiple SIgnal Classification ALgorithm is an intensity fluctuation-based nanoscopy algorithm used to get the superresolution in fluorescence microscopy when the object is diffraction-limited. This article establishes an innovative combination of QPI and MUSICAL, referred to as MusiQ where "Musi" stands for the MUSICAL and 'Q' stands for the QPI. The MusiQ can trace the motion patterns of spermatozoa with nanoscale details using low numerical aperture (NA) label-free QPI of sperms in motion and is therefore compatible with ARTs.

In the presented approach, high contrast raw image stream of moving sperms is acquired using a partially spatially coherent digital holographic microscope (optical setup in Supplemental Fig. 1, available online), and phase reconstruction is performed on each frame to obtain QPI image stream from the raw data stream of the microscope. Thereafter, an entire stream of QPI images is processed using MUSICAL to obtain nanoscale motion traces of all the sperms in the FOV. The workflow of MusiQ is given in Supplemental Figure 2.

The motion traces derived using MusiQ show nanoscale details that are suppressed by conventional motion tracing approaches used in the CASA solutions (13, 14, 20). Further, MusiQ does not make any assumption regarding the motion pattern for tracing the motion trace, as opposed to other recent particle tracking-based techniques (13, 14, 20). Lastly, MusiQ can derive the motion traces of all the sperms in a FOV of the QPI microscope in one execution.

Once the motion traces are formed, we computed kinematic features for individual sperms as a postprocessing step. We used the kinematic features to assess if they provide complementary information over conventional tests of progressive motility and permitted further distinction among progressively motile sperms regarding the regularity in motion patterns. Furthermore, we saw that seeing all the motion traces together facilitated qualitative assessment of the overall sample or individual sperms through visual inspection. We found that the same workflow can be used for all varieties of sperm cells in a semen sample and for sperm samples from patients with different fertility conditions.

MATERIALS AND METHODS

Sample preparation

To perform the experiment for QPI, the semen sample was deposited on top of a reflecting silicon chip. To prepare the sample, we first clean the silicon wafer chip in a mixture of 5% Helmanex, and 95% deionized water at 75°C for 10–15 min. It is followed by immersion in acetone and isopropanol and finally dried with nitrogen gas. To maintain sparsity between the sperm cells, we diluted the sample with 5:320 μL (Cell: phosphate buffered saline) using the micropipettes. The sample was prepared on a custom sample holder made up of a rectangular hollow chamber of polydimethylsiloxane over top of the silicon wafer to restrict the axial extent of motion and sealed with a 0.17 mm thick coverslip so that the sample homogeneously spread over the chip. The fresh sperm samples were collected from the different patients who came for routine analysis before starting assisted reproduction in the IVF clinic in the Department of Obstetrics and Gynecology, University Hospital of North Norway, Tromsø, Norway, and a portion of the sample has been used for the study and transferred to the Department of Physics and Technology, UiT Norway for experimentation. All subjects have voluntarily given written informed consent to be part of the study. All sperm samples were anonymized by removal of direct patient identifiers, before nanoscale motion tracing of spermatozoa.

MusiQ

A digital holographic microscopy system is used for the experimentation. Quantitative phase imaging system is used to measure the raw interferometric data in a video format, which is then processed using the Fourier space phase reconstruction technique to derive the phase map video. The reconstructed unwrapped phase maps over time are used as label-free datasets for the motion trace analysis. The choice of system and reconstruction approach ensures the possibility of single-shot,

high-speed imaging. This phase map video is processed using MUSICAL. Usually, ≥50 frames should be used, but in principle, there is no upper limit on the number of frames. We use the following rule of thumb to determine the minimum number of frames. Suppose we want to study motion patterns for sperms of progressive motility with a speed more than v μm/s over at least n helical periods which have an average length of d μm. Suppose the acquisition rate of the camera is f frames/s, and then the required minimum number of frames is ndf/v. Validation of MusiQ as a label-free motion tracing approach is performed on a nonbiological benchmark sample of a bead guided on an optical waveguide (21). This validation is presented in the Supplemental Note 1 (available online) and Supplemental Figure 3 using systems described in Supplemental Figures 7 and 8.

Quantitative phase imaging

The schematic diagram of the experimental setup for the proposed study is shown in Supplemental Figure 1. A diode-pumped solid-state laser (Cobolt Flamenco, $\lambda = 660$ nm, Cobolt AB, a part of HÜBNER Photonics, Solna, Sweden) passes through a rotating diffuser, a microscope objective (MO1), and a large core multimode fiber to reduce the spatial coherence of the light source (22, 23). The output of the multimode fiber is treated as an extended incoherent light source exhibiting partial spatial coherence, i.e., high temporal but low spatial coherence (24). The choice of partial spatial coherence is motivated by the fact that spatial coherence produces a speckle pattern as shown in Supplemental Figure 1A which degrades the image quality and reduces the phase sensitivity of the system. The use of partially coherent illumination eliminates speckles, as shown in Supplemental Figure 1B. The output of the multimode fiber is used as an input of a Linnik interferometer. Lens L1 (f = 50 mm), collects the incident light beam and collimates it to the back focal plane of lens L2 (f = 150 mm). Lens L2 focuses the light beam at the back aperture plane of two identical MO2 and MO3 after passing through a 50/50 beam splitter. The beam splitter divides the incident beam into two parts, one toward the sample arm and another toward the reference arm. In the reference arm, we place a slightly tilted mirror to get the tilted plane wavefront as a back reflection from the reference. The back-reflected light from the reference arm interferes with the back-reflected light from the sample at the beam splitter. The interference signal is recorded to the camera (Dhyana, Tucsen, China, China) plane using a tube lens L3 (f = 200 mm). The mathematical model and phase map reconstruction for our system are detailed in Supplemental Methods 1 (available online).

We measured the spatial phase sensitivity of the system, i.e., the spatial phase noise of the system for phase imaging, as follows. We placed a flat mirror of flatness $\lambda/10$ as the sample under the microscope and acquired an interferometric image. The reconstructed phase of the flat mirror ideally should be 0, but environmental vibrations cause fluctuations that make the system unavoidably unstable. The average spatial phase sensitivity of our system is ± 20 mrad, as shown in Supplemental Figure 1C.

MUSICAL for motion tracing

The detailed description, mathematics, and discussion about MUSICAL can be found in (15) and provided in Supplemental Methods 2. The adaptation of MUSICAL for motion analysis using phase maps does not require algorithmic modification but requires modification of the optical parameters used in MUSICAL's implementations (16). In fluorescence microscopy, the point-spread-function of the system can be estimated using the actual optical parameters of the system such as NA. However, in MusiQ, the NA cannot directly be used in MUSICAL because the bandwidth is reduced because of phase retrieval while performing QPI. We therefore experiment with different effective NAs, all lower than the NA of the actual microscope objective lens, and use the NA that produces the sharpest images. The remaining parameters such as pixel size and emission can be used directly. MusiJ plugin (16) is used to generate MUSICAL images. For the sperm sample, the parameters used were wavelength 660 nm, pixel size 650 nm, magnification 1, and effective NA of 0.15 (lesser than the system actual NA of 0.25 because of the reduction in the Fourier transform phase retrieval bandwidth).

Straight-line velocity (referred to as speed)

We calculated the straight-line velocity for the progressive sperms considering a section of the motion pattern where the helical path is relatively along a straight line. The expression for computing the magnitude of this straight-line velocity is

$$V_{normal} = \frac{||r_{end} - r_{start}||}{N_f \tau_e} \quad (1)$$

where r_{end} and r_{start} are the end and start frames positions in the linear section of the motion trace considered for computing this parameter. N_f is the number of frames spanning the linear section and τ_e is the exposure time per frame. Different studies have been performed in the past to quantify the straight-line velocity of normal cells to improve the prediction of successful IVF or ICSI therapies (13, 25). Studies suggest that an average straight-line velocity of 25 μm/s is needed for successful IVF therapies (25). For the convenience of reference, we refer to the linear velocity magnitude expressed in equation (1) as simply the speed of the sperm.

Kinematical features of sperm motion traces

Here, we present examples of four features. These features are derived by splitting the motion trace of a sperm into individual segments, e.g., one period of the helical motion pattern. Each segment can be fit by a rectangular box as shown in Figure 1A with the precision given by the MusiQ image's resolution. The dimensions of each rectangular segment indicate the length of the helical path (being referred to as the period here) and twice the radius of the helical path. Then statistics can be computed over all the segments of the motion trace

FIGURE 1

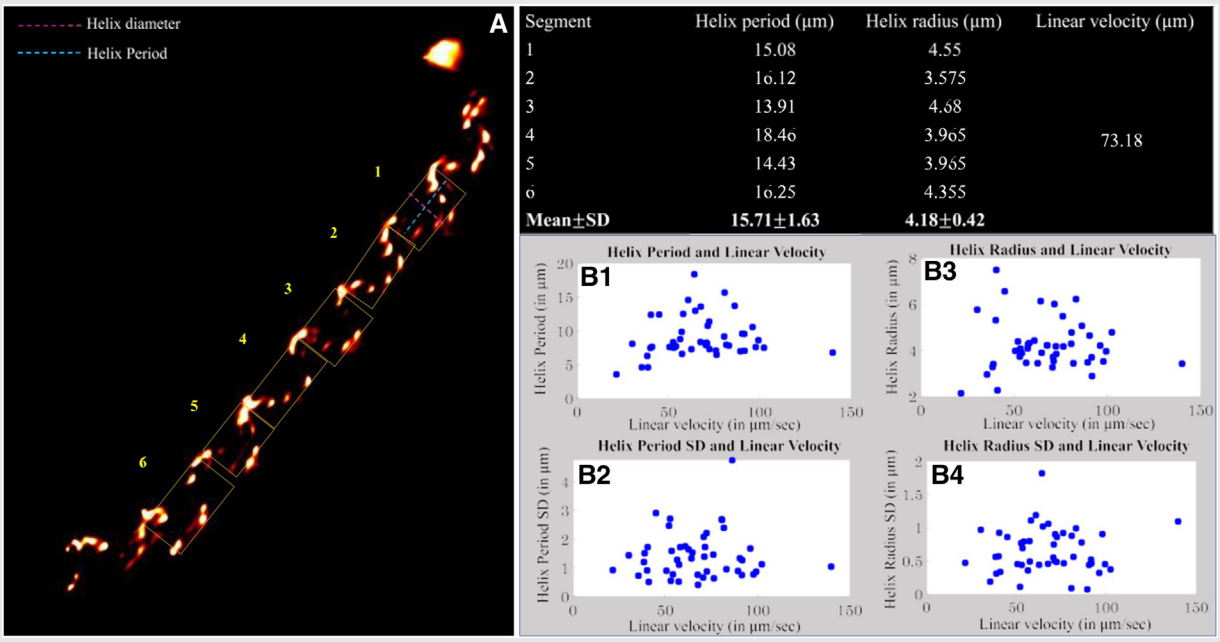

Nanoscale motion tracing of the sperm cells offers subdiffraction features. (**A**) Different box shows variations in radius and period during the motion of the cell. Period ± standard deviation and radius ± standard deviation of these segments are shown in the table. (**B**) These features are plotted against the linear velocity of the cells.

Bhatt. Motion consistency of spermatozoa. F S Sci 2024.

of a given sperm. Here, we compute the mean and standard deviation of their periods, and similarly of their radii. Each of these four values is a new kinematic feature of a progressive sperm.

RESULTS

Nanoscale motion reconstruction

We use a QPI system with a low NA (×10, 0.25 NA) objective lens to obtain phase maps at different time instances as described in the methods section. Examples of such temporal phase maps are shown in Figure 2 A1–A6. MUltiple SIgnal Classification ALgorithm is then applied, and the MusiQ result is shown in Figure 2A.

Tracing the motion pattern with the maximum projection of phase maps is shown in Figure 2B. It can show the helical motion of the sperm cells. Nonetheless, the motion traces derived using MUSICAL shown in Figure 2A has significantly finer details than the motion pattern derived by maximum projection of the phase maps shown in Figure 2B.

In the quantitative sense, for the chosen optics (10x, 0.25 NA) and the chosen Fourier space phase reconstruction technique, the diffraction-limited resolution is 1,320 nm. In comparison, the resolution obtained by MusiQ is of the order 340 nm. We considered the use of other superresolution techniques instead of MUSICAL. A detailed study was performed and is presented in Supplemental Note 2 and Supplemental Figures 4 and 5. The relevant supplementary methods are presented in Supplemental Methods 3. Note that the Stochastic Optical Reconstruction microscopy localizations collected over time are the high-precision equivalent of particle tracking algorithms used in conventional CASA. The study shows that MUSICAL has a larger bandwidth in the Fourier spectrum and higher Fourier intensity at high-frequency components than the other methods, which indicates superior resolution support of MUSICAL. The study also demonstrates MUSICAL's ability to present the motion trace in high contrast and with fewer artifacts than the other methods.

We also considered the utility of another label-free imaging technique, namely the bright field microscopy, which is quite popularly used in fertility clinics for its simplicity of interpretation by humans. The representative brightfield images in Figure 2C1–C6 clearly indicate good visual interpretability of sperms at individual time instances. The results of applying MUSICAL and performing maximum projection are shown in Figure 2C and D and present high artifact-prone motion traces, which are qualitatively much poorer than both Figure 2A and B. A discussion related to it and other common label-free techniques is presented in Supplemental Note 3.

In addition, we show the motion trace analysis of sperm cells with large field-of-view (FOV) in Supplemental Figure 6. It is important to analyze and identify the quality of sperm cells over large FOV for ICSI and IVF. We demonstrate the effectiveness of MusiQ on full FOV and also present the counts of progressively motile, motile, and immotile sperms. Our current FOV can support imaging and motion tracing of 35–40 sperms already. The present analysis can be upgraded by integrating larger camera chipsets that have 4–16 times larger FOV, supporting a large statistical sample pool per FOV.

FIGURE 2

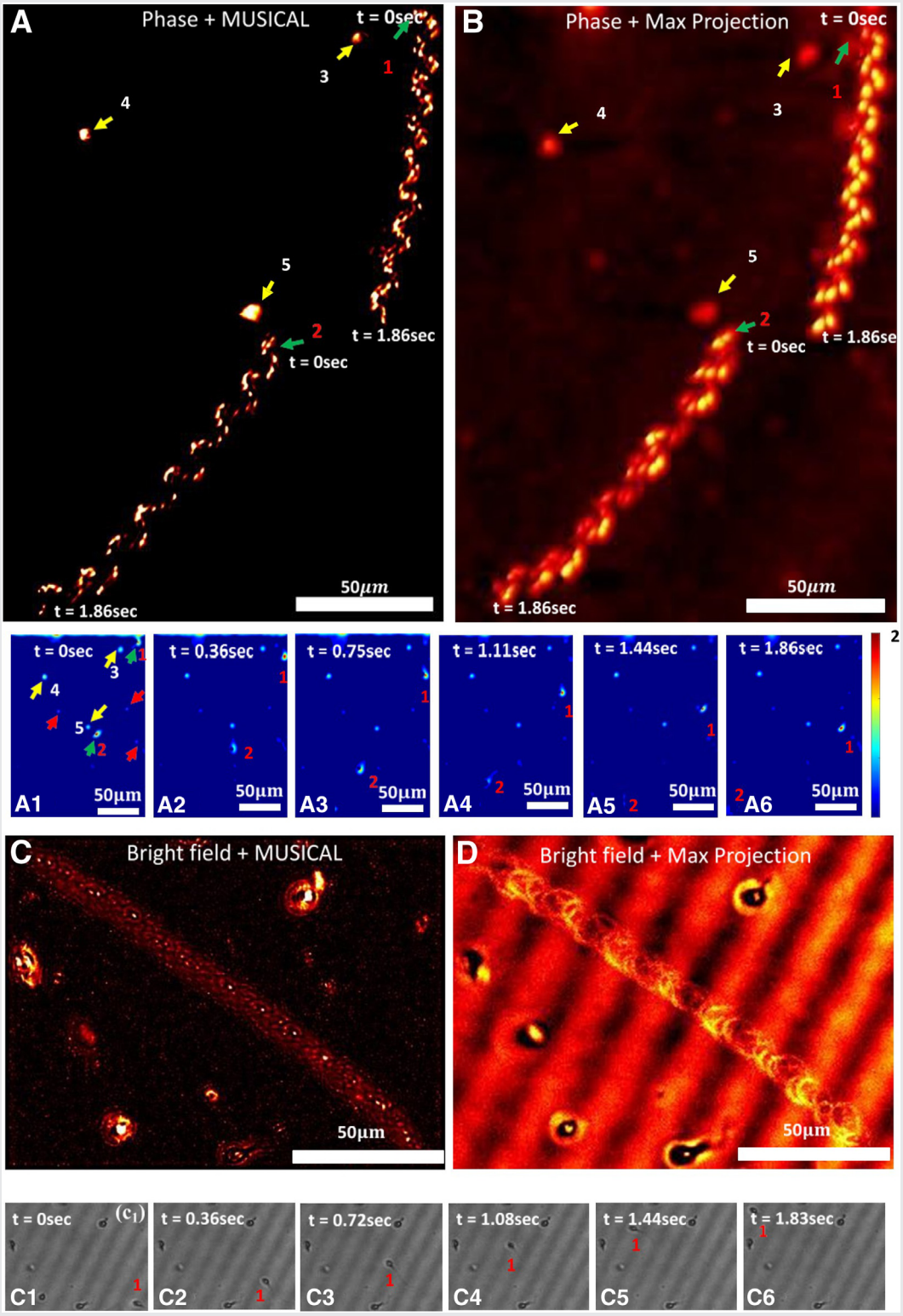

Motion tracing of sperms using a different approach. (**A**) Proposed phase imaging with MUSICAL shows ×3 fine motion tracing of the cells compared with the maximum projection (**B**) of the phase images. On the other hand, (**C**, **D**) motion tracing with bright field images is unable to show the fine motion features. In our analysis, green arrows represent normal sperm cells (progressive cells) tracing the helical path in a straight line. Yellow arrows show nonprogressive sperm cells moving in a close vicinity. Red arrows represent immotile (dead) cells with very low phase and amplitude contrast. On the other hand, conventional microscopy techniques are not capable of tracing the precise motion of the cells. MUSICAL = MUltiple SIgnal Classification ALgorithm.

Bhatt. Motion consistency of spermatozoa. F S Sci 2024.

Nanoscale details provide complementary features to the speed of spermatozoa

It is interesting to note that dead sperms or debris (red arrows in Figure 2A1) do not experience any motion at all, and therefore they are absent from the MusiQ image completely as seen in Figure 2A. Immotile sperms may have almost no motion, therefore they either do not appear in the MusiQ image or appear as very small dots. Furthermore, sperms that are motile but not progressive experience short spurs of motion or local motion in small confinements (26). Such sperms are indicated using yellow arrows in Figure 2A1. They appear as large dots in the MusiQ image as shown in Figure 2A. Therefore, MusiQ works as an automatic computation filter for all types of nonprogressive sperms.

However, the most exciting feature of the MusiQ traces of progressively motile sperms is the nanoscale details in their motion pattern. This presents an opportunity to design new features with fine precision, which can complement the existing features such as speed and direction of the motion of sperm. We designed four new kinematic features assuming that high-quality progressive motile sperms present a regular and consistent helical motion pattern. These are the mean of the helix period, standard deviation of the helix period, mean of helix radius, and standard deviation of helix radius. The procedure to extract these features is presented in the methods section. An illustration of these statistical features is given in Figure 1A.

We analyzed multiple FOVs which contained a total of 47 progressively motile sperms which all have speed (a straight-line velocity magnitude described in the methods section) of >25 μm/s, as recommended for IVF and ICSI (25). Motion tracing of the progressive sperm cells shows that while moving in the forward direction, these cells experience changes in the periodicity and radius of the helical path. We plotted the four new features against the straight-line velocity magnitude of the sperms. It is seen that none of these features correlated with the speed of the sperms. This implies that these features contribute additional complementary information to the speed of the sperms. More illustrative examples are given in Figure 3.

Variation in nanoscale patterns may have insight into motion consistency and sperm quality

Here, we present examples of how the features can be used for further insight into qualitative aspects that can differentiate progressive sperms and indicate factors of quality. A scatter plot of the standard deviation of periods and the standard deviation of the radii is shown in Figure 3. Our motion analysis can resolve finer motion details that lie under the diffraction limit and therefore cannot be resolved using conventional motion tracing analysis. All blue dots under the red box shown in Figure 3 contained diffraction-limited features while all of them are not optimal for fertilization.

We select five sperms, each with speed of >50 μm/s, and therefore conventionally representing high-quality sperms. Barring the criterion regarding speed, the selection of these sperms was performed randomly. Their motion traces are presented also in Figure 3, and they are assigned identifiers (IDs) A–E. Besides the motion traces, the value of speed and the four features described above are presented. In the conventional sense, speed is representative of the quality of sperm (13, 25). Accordingly, the sperms arranged in the decreasing order of speed are B, C, E, D, and A. We now analyze their motion traces qualitatively and their nanoscale feature values quantitatively.

Although sperm ID B is the fastest (>80 μm/s), a quick view of the motion trace of sperm ID B is sufficient to indicate that this sperm does not demonstrate a regular helix pattern. It is also seen that sperm ID B's standard deviation of periods lies outside the red box. The irregularity is also seen in the high standard deviation of its period (approximately 2.7 μm/s).

The next sperm in terms of speed is sperm ID C (>70 μm/s). Its motion pattern indicates that its motion is not quite helical. Although the current work does not include a measure of helicity as one of the features, such a feature can be designed in the future. Beyond this quick qualitative and visual interpretation, the standard deviations of both the periods and radii are high. This is especially true for the standard deviation of the radii, which is the highest for sperm ID C in comparison to the rest except sperm ID E.

The next sperm is sperm ID E (speed >65 μm/s). Sperm ID E has the highest standard deviation of radii. However, the motion trace of this sperm clearly indicates a high-quality helical motion, although with a tapering radius. Potentially, the gradient of radii is also an interesting indicator of the quality and may become one of the features engineered in the future. In addition, this sperm has the lowest standard deviation of periods (indicating regularity in the helical pattern). Therefore, it is likely that this sperm has a high-quality in terms of regularity of the pattern.

The next sperm in sperm ID D (speed >52 μm/s). Although its speed is among the lowest of the five chosen sperms, we see that its standard deviations of both period and radii are toward lower values. This indicates regularity in the helical motion. This regularity is also qualitatively evident in its motion trace. Therefore, sperm ID D may in fact be the sperm with the most consistency in its motion, which may also indicate a superior mitochondrial mechanism in comparison with the other sperms (27).

The slowest sperm among the five selected here is sperm ID A. It is the second highest in terms of the standard deviation of the period, indicating irregularity of helical motion. This is also indicated in the nanoscale motion trace, although the evidence is not conclusive. On the basis of the experimental evidence, it may not be of as high-quality as sperms with IDs D and E. We note that this sperm is from a FOV which was imaged for the longest duration. Therefore, its statistical features may be more reliable than most. Instead, it may indicate that the statistics should be derived for smaller time windows and their variations across time may also be insightful.

Motion trace analysis for fertility patients with normal and abnormal sperm cell conditions

The use of CASA is generally restricted to sperm cells in normal patients. The reasons include insufficient contrast and edge artifacts presented by the conventional imaging techniques discussed before; inapplicability of the shape

FIGURE 3

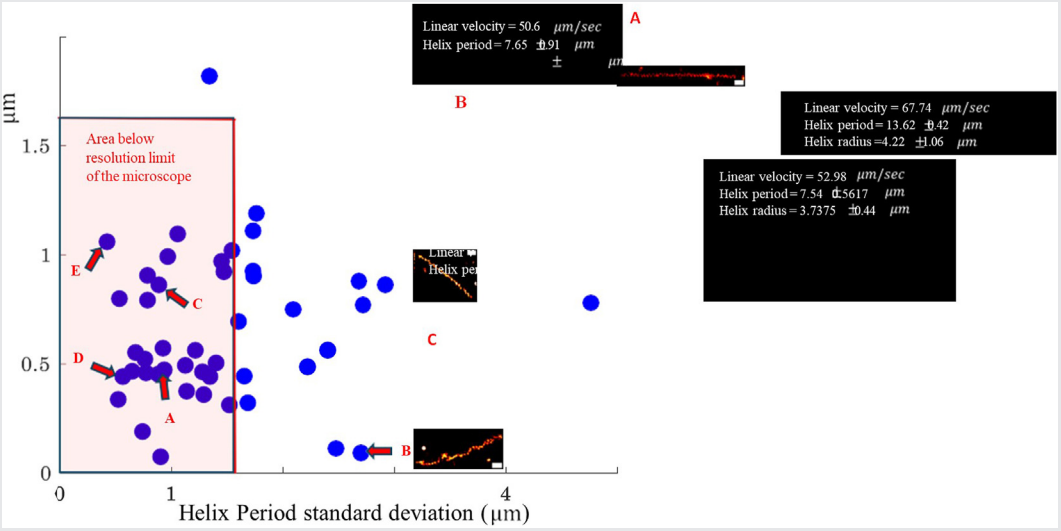

Scatter plot between the standard deviation of the periods and the standard deviation of the radii of individual sperms. Motion traces of five random sperms that fulfill the criteria for progressive motility (i.e., speed >25 μm/s) are shown here.

Bhatt. Motion consistency of spermatozoa. F S Sci 2024.

and motion models used in CASA to the abnormal sperm cells, such as with abnormally small or big head or tail, more than one tail, nonhelical motion pattern, etc.; and limited ability to derive model-free motion trace of sperms. Quantitative phase imaging resolves this issue, as shown in (13, 28) as well as proven here. But, the second and third points have remained a bottleneck. However, our MusiQ solution overcomes these issues as we show here.

We applied MusiQ on the semen sample from a patient with a known pathological condition that manifests as abnormal sperm cells (diagnosis established using genetic testing and morphological analysis under an electron microscope), affecting both the morphology and motility of the cells. The exact condition is not mentioned for protecting the personal identity of the patient. The results are presented in Figure 4. Motion traces of sperms from another patient with normal sperm cells are also provided in Figure 4 for reference. It is easy to see that the sample with abnormal sperm cells demonstrates significant curvilinear motion patterns and no visible helical motion pattern. The trace of abnormal cells is also not relatively straight, therefore lacking direction. This result not only shows that the proposed MusiQ solution can be applied to patients with both normal and abnormal semen samples, but the availability of the motion traces also indicates a potential to design quantitative features for abnormal sperm cells even without assuming a motion model in the future. Further, we show the motion trace analysis of low-quality sperm cells in Supplemental Figure 9. We have used a total of 3–5 patient samples and one prefiltrated low-quality semen sample for validation in our study.

DISCUSSION

Computer-aided semen analysis at present is primarily used for semen analysis and not selection of specific sperms for fertilization. The primary obstacle is the ability to perform live analysis for several sperms swimming at a variety of speeds, identification of the sperms suitable for fertilization, and automation of selection or isolation of the better sperms. There is number of techniques developed in the past for sperm retrieval from patients with obstructive and nonobstructive azoospermia (6–8, 29–37). To our knowledge embryologists in most laboratories worldwide have a subjective manual selection method using phase contrast imaging for the choice of morphologically normal sperm cells for microinjection. In addition, recently, several techniques have been used for tracking the motion of spermatozoa and providing motion trace analysis (14, 20). The study (20), reconstruction adds quantitative parameters for clinical use or biomedical experiments, providing 4-dimensional viewing for a more informed selection of sperm cells. In addition, (14) offers the reconstruction of the 3-dimensional motion of freely moving sperms, including their head translation, rotation/spin, and flagellar beating patterns, which could be beneficial for biological and biophysical studies. Nonetheless, these study offers diffraction-limited motion tracing while MusiQ could be used for the filtration of a high-quality sperm cell on the basis of nanoscale motion trace with finer details and kinematic features. This work indicates that the motion of several sperms can be analyzed together to contribute supplementary kinematic features that may assist in

FIGURE 4

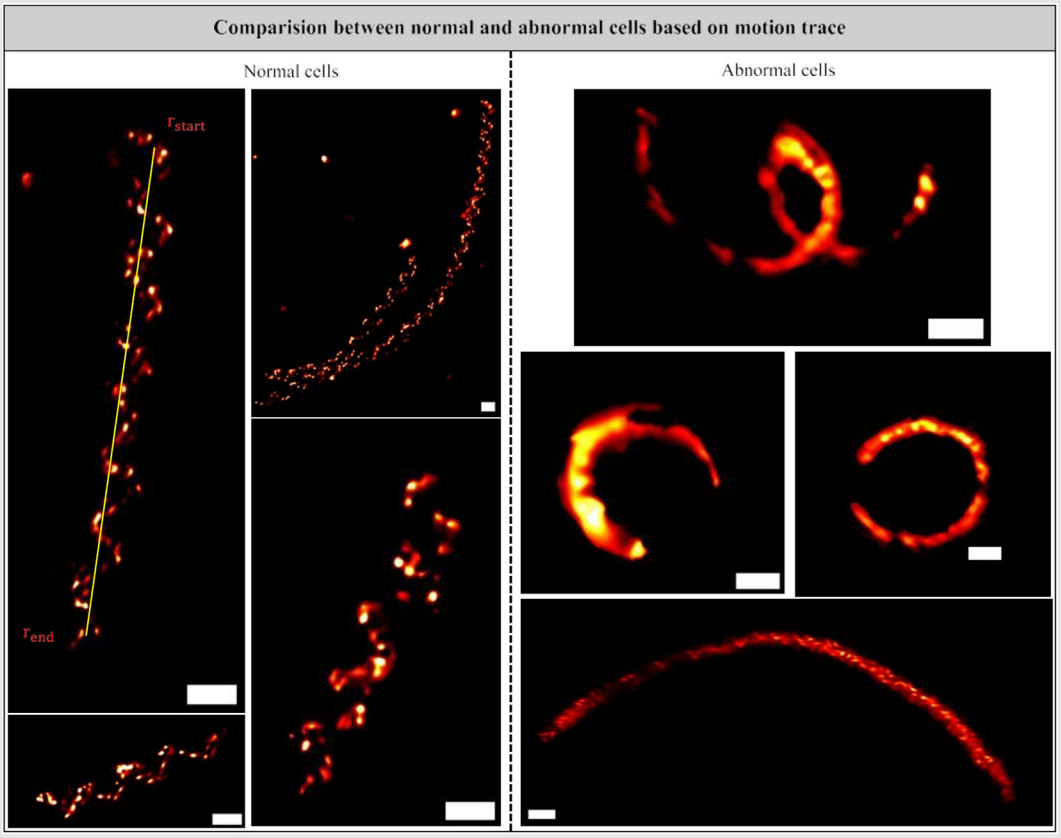

Motion trace of different normal (high-quality) and abnormal (low-quality) cells on the basis of the proposed label-free MusiQ. Bar = 10 μm.

Bhatt. Motion consistency of spermatozoa. F S Sci 2024.

discriminative selection of better suited sperms among all the good ones.

Yet, the current literature does not specify the qualities of sperms best suited for fertilization, and the skilled clinicians choose them heuristically. A discussion with several such clinicians indicates speed, directionality, and regularity of motion as their main criteria, although all of them admit that it is difficult to visually assess all these criteria when manually selecting the best sperms. We suppose that a systematic large-scale study should be designed to identify the characteristics of sperms with the highest likelihood of fertilization, and further to the likelihood of viability and implantation success.

MusiQ opens the potential to design a variety of kinematic features. In this work four such features and indicated, and the utility of two of them has been shown. These two features are the standard deviation of the periods and the standard deviation of the radii of helical segments of sperms. Further, the potential of exploring other features such as gradient of radii, helicity, etc. is also indicated. Identification of the most suitable kinematic features needs identification of the characteristics of the best suited sperms, as discussed in the previous paragraph.

We plan to work on large-scale studies with fertility scientists to identify and engineer quantitative features that support finer quality analysis of the sperms and facilitate advanced CASA which can be even more selective and helpful in identifying sperms better suited for fertilization. Another future plan is to enable real-time phase reconstruction, MUSICAL, and nanoscale feature analysis toward the realization of a clinically deployable advanced CASA for supporting IVF and ICSI.

We note that MUSICAL is an image analysis technique that may vaguely fall under the machine learning category, but the conventional metrics for reporting found in Enhancing the QUAlity and Transparency Of health Research network do not apply. Alternative suitable metrics are reported, and bias is avoided through random selection of regions for analysis. Detailed methods are included in the supplementary notes for reproducibility.

CONCLUSION

In this article, we demonstrate MusiQ for nanoscale motion tracing as a supplementary tool for sperm quality analysis on the basis of nanoscale details in their motion patterns. The studies provide the proof of concept that a unique integration of a high contrast label-free imaging method and a superresolution computational approach presents valuable insights into the kinematic features of sperm cells. MusiQ

presents the opportunity to design new features for quality differentiation among the progressive sperms.

The ability to image motion patterns of both normal and abnormal morphology and motion behavior is demonstrated. Further, the potential of large FOV analysis is also shown. The techniques used in MusiQ are low dose and not phototoxic to sperms, as they use the light source and dosage used in microscopes in the fertility clinics, e.g., for ICSI. Therefore, MusiQ does not pose any additional risk to sperm health. However, further large-scale studies are needed to identify the characteristics of sperms that give them a competitive advantage for fertilization, such that the most suitable nanoscale kinematic features can be designed.

Acknowledgments

The authors acknowledge Dilip Kumar Prasad, Ph.D. and Balpreet Singh Ahluwalia, Ph.D. for discussions.

CRediT Authorship Contribution Statement

Sunil Bhatt: Acquired the raw microscopy data, Computed the kinematic features, Formal analysis. Ankit Butola: Conceptualization, Methodology, Study design, Supervision. Sebastian Acuña: Computed the motion traces from the phase maps. Daniel Henry Hansen: Instrumentation. Jean-Claude Tinguely: Instrumentation. Mona Nystad: Provision of sperm samples and insights. Dalip Singh Mehta: Provided primary salary (to Sunil Bhatt), Supervision. Krishna Agarwal: Conceptualization, Methodology, Study design, Supervised entire project, Supported all the resources except the sperm samples.

Declaration of Interests

S.B. has nothing to disclose. A patent application containing the idea and application of this work as a subset of the claims has been submitted, where A.B. and K.A. are coinventors. They have not received any monetary gains pertaining this. They have received funding from European Research Council and Forskningsradet for commercialization of the patented technology; University hospital of North Norway UNN's fertility clinic provided anonymized and centrifuged sperm samples. S.A. has nothing to disclose. D.H.H. has nothing to disclose. J.-C.T. has nothing to disclose. M.N. has nothing to disclose. D.S.M. has nothing to disclose. K.A. reports European Research Council Starting grant 804233 and European Research Council PoC 101123485 that funded the study.

REFERENCES

1. Van Waart J, Kruger TF, Lombard CJ, Ombelet W. Predictive value of normal sperm morphology in intrauterine insemination (IUI): a structured literature review. Hum Reprod Update 2001;7:495–500.
2. Farquhar C, Marjoribanks J, Brown J, Fauser BC, Lethaby A, Mourad S, et al. Management of ovarian stimulation for IVF: narrative review of evidence provided for World Health Organization guidance. Reprod Biomed Online 2017;35:3–16.
3. Van Steirteghem AC, Nagy Z, Joris H, Liu J, Staessen C, Smitz J, et al. High fertilization and implantation rates after intracytoplasmic sperm injection. Hum Reprod 1993;8:1061–6.
4. Raveshi MR, Abdul Halim MS, Agnihotri SN, O'Bryan MK, Neild A, Nosrati R. Curvature in the reproductive tract alters sperm–surface interactions. Nat Commun 2021;12:3446.
5. Hu W, Zhu Y, Wu Y, Wang F, Qu F. Impact of COVID-19 pandemic on the pregnancy outcomes of women undergoing assisted reproductive techniques (ARTs): a systematic review and meta-analysis. J Zhejiang Univ-Sci B 2022;23:655–65.
6. Baldini D, Ferri D, Baldini GM, Lot D, Catino A, Vizziello D, et al. Sperm selection for ICSI: do we have a winner? Cells 2021;10:3566.
7. Vaughan DA, Sakkas D. Sperm selection methods in the 21st century. Biol Reprod 2019;101:1076–82.
8. Cherouveim P, Velmahos C, Bormann CL. Artificial intelligence for sperm selection–a systematic review. Fertil Steril 2023;120:24–31.
9. Finelli R, Leisegang K, Tumallapalli S, Henkel R, Agarwal A. The validity and reliability of computer-aided semen analyzers in performing semen analysis: a systematic review. Transl Androl Urol 2021;10:3069–79.
10. Mortimer ST, Van der Horst G, Mortimer D. The future of computer-aided sperm analysis. Asian J Androl 2015;17:545–53.
11. Butola A, Popova D, Prasad DK, Ahmad A, Habib A, Tinguely JC, et al. High spatially sensitive quantitative phase imaging assisted with deep neural network for classification of human spermatozoa under stressed condition. Sci Rep 2020;10:13118.
12. Dubey V, Popova D, Ahmad A, Acharya G, Basnet P, Mehta DS, et al. Partially spatially coherent digital holographic microscopy and machine learning for quantitative analysis of human spermatozoa under oxidative stress condition. Sci Rep 2019;9:3564.
13. Su TW, Xue L, Ozcan A. High-throughput lensfree 3D tracking of human sperms reveals rare statistics of helical trajectories. Proc Nat Acad Sci U S A 2012;109:16018–22.
14. Daloglu MU, Luo W, Shabbir F, Lin F, Kim K, Lee I, et al. Label-free 3D computational imaging of spermatozoon locomotion, head spin and flagellum beating over a large volume. Light Sci Appl 2018;7:17121.
15. Agarwal K, Macháň R. Multiple signal classification algorithm for super-resolution fluorescence microscopy. Nat Commun 2016;7:13752.
16. Acuña S, Ströhl F, Opstad IS, Ahluwalia BS, Agarwal K. MusiJ: an ImageJ plugin for video nanoscopy. Biomed Opt Express 2020;11:2548–59.
17. Butola A, Acuña S, Hansen DH, Agarwal K. Scalable-resolution structured illumination microscopy. Opt Express 2022;30:43752–67.
18. Sekh AA, Opstad IS, Birgisdottir AB, Myrmel T, Ahluwalia BS, Agarwal K, et al. Learning nanoscale motion patterns of vesicles in living cells. In: Proceedings of the IEEE/CVF Conference on Computer Vision and Pattern Recognition; 2020:14014–20.
19. Yu J, Wu C, Sahu SP, Fernando LP, Szymanski C, McNeill J. Nanoscale 3D tracking with conjugated polymer nanoparticles. J Am Chem Soc 2009;131:18410–4.
20. Dardikman-Yoffe G, Mirsky SK, Barnea I, Shaked NT. High-resolution 4-D acquisition of freely swimming human sperm cells without staining. Sci Adv 2020;6:eaay7619.
21. Bhatt S, Butola A, Acuña S, Hansen DH, Tinguely J-C, Mehta DS, et al. Quantitative phase imaging for tracing the motion of waveguide trapped bead particle. In: Imaging, Manipulation, and Analysis of Biomolecules, Cells, and Tissues XXI. SPIE; 2023:19–26.
22. Bhatt S, Butola A, Kumar A, Thapa P, Joshi A, Jadhav S, et al. Single-shot multispectral quantitative phase imaging of biological samples using deep learning. Appl Opt 2023;62:3989–99.
23. Butola A, Kanade SR, Bhatt S, Dubey VK, Kumar A, Ahmad A, et al. High space-bandwidth in quantitative phase imaging using partially spatially coherent digital holographic microscopy and a deep neural network. Opt Express 2020;28:36229–44.
24. Bhatt S, Butola A, Thapa P, Saxena A, Ahmad A, Mehta DS. Partially spatially coherent light-based multispectral quantitative phase microscopy. In: Optics and the Brain. Washington, DC: Optica Publishing Group; 2022:JTu3A.
25. Michelmann HW. Minimal criteria of sperm quality for insemination and IVF therapy. Int J Androl 1995;18(Suppl 1):81–7.

26. World Health Organization. WHO laboratory manual for the examination and processing of human semen. 5th ed. Geneva, Switzerland: WHO Press; 2010.
27. Irigoyen P, Pintos-Polasky P, Rosa-Villagran L, Skowronek MF, Cassina A, Sapiro R. Mitochondrial metabolism determines the functional status of human sperm and correlates with semen parameters. Front Cell Dev Biol 2022; 10:926684.
28. Nygate YN, Levi M, Mirsky SK, Turko NA, Rubin M, Barnea I, et al. Holographic virtual staining of individual biological cells. Proc Natl Acad Sci U S A 2020;117:9223–31.
29. Bibancos M, Vaz RM, Mega PF, Borges E Jr, Ribeiro M, Buttros D, et al. Sperm selection for micro TESE-ICSI in non-obstructive azoospermia, a case report. JBRA Assisted Reprod 2021;25:653–6.
30. Ezeh UI, Moore HD, Cooke ID. A prospective study of multiple needle biopsies versus a single open biopsy for testicular sperm extraction in men with non-obstructive azoospermia. Hum Reprod 1998;13:3075–80.
31. Harrison RAP. A highly efficient method for washing mammalian spermatozoa. J Reprod Fertil 1976;48:347–53.
32. Jeyendran RS, Van der Ven HH, Perez-Pelaez M, Crabo BG, Zaneveld LJ. Development of an assay to assess the functional integrity of the human sperm membrane and its relationship to other semen characteristics. J Reprod Fertil 1984;70:219–28.
33. Lopata A, Patullo MJ, Chang A, James B. A method for collecting motile spermatozoa from human semen. Fertil Steril 1976;27:677–84.
34. Lo Monte G, Murisier F, Piva I, Germond M, Marci R. Focus on intracytoplasmic morphologically selected sperm injection (IMSI): a mini-review. Asian J Androl 2013;15:608–15.
35. World Health Organization. WHO laboratory manual for the examination and processing of human semen. World Health Organization; 2021.
36. Smith GD, Takayama S. Application of microfluidic technologies to human assisted reproduction. Mol Hum Reprod 2017;23:257–68.
37. Vermey BG, Chapman MG, Cooke S, Kilani S. The relationship between sperm head retardance using polarized light microscopy and clinical outcomes. Reprod Biomed Online 2015;30:67–73.